DISTRIBUTION OF HYDROTHERMAL VEINS IN CHICXULUB CRATER IMPACT BRECCIAS. E. T. Blom[1,2] and D. A. Kring[2], [1]University of Chicago, 5734 S Ellis Ave, Chicago, Illinois 60637, [2]Lunar and Planetary Institute, USRA, 3600 Bay Area Blvd, Houston, Texas 77058.

Introduction: The ~180 km diameter Chicxulub impact crater [1] is Earth's largest and best-preserved peak-ring basin. Multiple lines of evidence indicate the extreme energy of impact generated an ~3-km-thick region of molten rock at the crater's center [2]. Heat from this central melt sheet may have promoted hydrothermal circulation up to 2.3 Ma after the impact event [3,4]. The crater's peak ring, which consists of highly fractured and porous impact breccias [5-7,3] and was directly adjacent to the melt sheet, would have been an ideal area for hydrothermal fluid flow.

Evidence of hydrothermal circulation at Chicxulub was first detected in two boreholes between the peak ring and the crater rim [3,4,8-12]. In 2016, the International Ocean Discovery Program (IODP) and International Continental Scientific Drilling Program (ICDP) Expedition 364 directly sampled the peak ring [13]. The expedition recovered core from 617 to 1335 meters below the sea floor (mbsf), including ~130 m of impact breccias and impact melt rocks that are the target of this study.

Methods: High resolution line-scan images of the core splits were taken during core logging at multiple light intensities and an average resolution of 14.8 pixels/mm. Additionally, computed tomography (CT) scans of the cores were conducted by Weatherford Laboratories for the expedition [14]. Line-scans and CT images from core section 41-1 to section 87-3 were analyzed in this study. ImageJ software was used to map the hydrothermal features observed in visible light line-scans and to calculate the areas of mapped features. Point counting was conducted to characterize the degree of alteration in seven core sections. Each count covered an area of 80 cm^2 with 2,000 points.

Results: Three distinct types of hydrothermal alteration features were recorded during the image analysis. A total of 89 green vein features were mapped between sections 41-1 and 51-2, characterized by a texturally-distinct dark gray to green matrix. From thin section analysis, green features are known to be primarily secondary calcite replacement [4]. Five orange veins were mapped in the analysis from section 52-1 through 54-1. Orange veins exhibit significant amounts of bright orange dachiardite-Na (hereafter dachiardite) and analcime in the vein matrix [4].

Regions of diffuse hydrothermal alteration were noted in association with both vein types, although alteration was significantly limited in green vein sections. The diffuse alteration was characterized by bright orange dachiardite in matrix pockets, along grain boundaries, and in clasts. Whereas the matrix in orange veins was nearly entirely replaced by dachiardite, the degree of dachiardite replacement in diffuse alteration regions was limited to 3% to 24%.

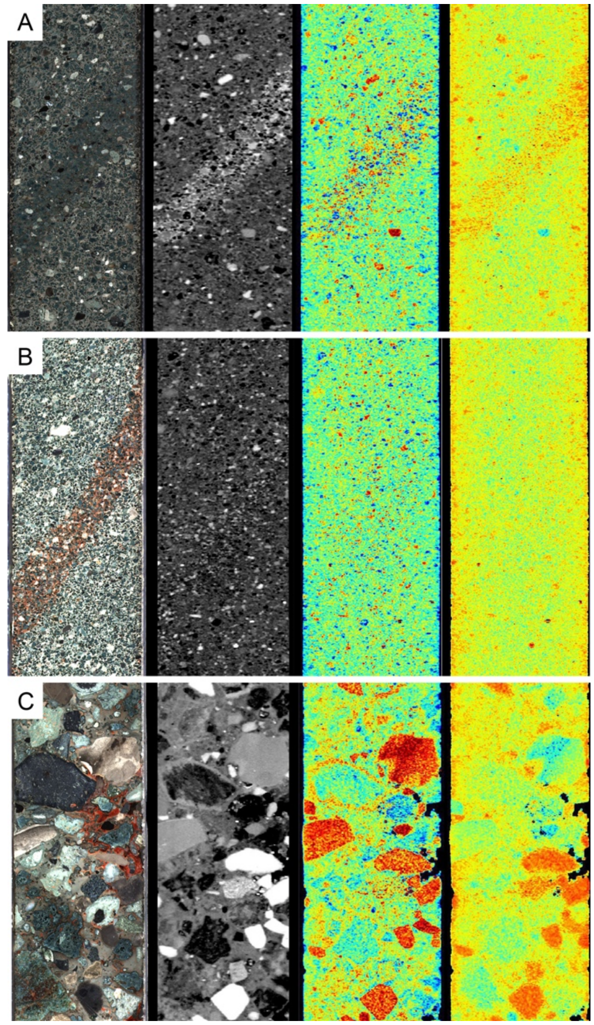

Figure 1. Examples of hydrothermal features. From left to right, images are provided in visible light, cleaned CT, bulk density, and effective atomic number. Displayed core area is 20 cm by 8.3 cm. (**A**) Green hydrothermal vein with matrix replaced by secondary carbonate. Sample 007A-48R-3, 50 to 70 cm (643 mbsf). (**B**) Orange hydrothermal vein with dachiardite replacement. Sample 0077A-54R-1, 48 to 68 cm (660 mbsf). (**C**) Region of diffuse hydrothermal alteration. Sample 0077A-63R-2, 60 to 80 cm (685 mbsf).

Discussion: As illustrated in Figure 2, green and orange vein features are found in distinct regions of the core with no overlap. The breccia in the lowest sections of green alteration and highest sections of of orange alteration are similar in matrix color and

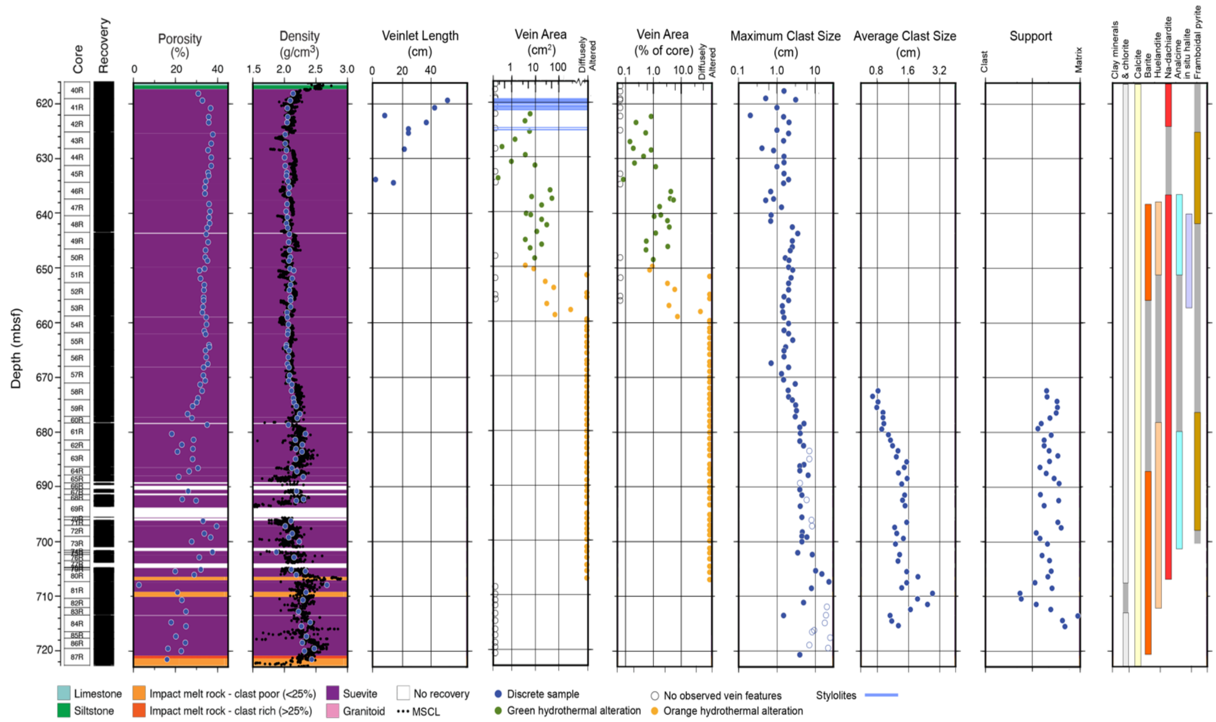

Figure 2 Porosity, density, hydrothermal vein area, maximum clast size, degree of matrix support, maximum clast size, length of veinlet features, and thin section mineralogy for core sections 40-1 through 87-3. All data are recorded at discrete sample depths (mbsf) with the exception of the black density data, which are downhole log data calibrated to wireline log depth below seafloor (WSF, m). Porosity, density, and maximum clast size data reproduced from [14], average clast size and support reproduced from [15], mineralogy reproduced from [4]. For the maximum clast size data, open circles indicate the largest clast extended beyond the boundary of the core. For the mineralogy data, colored regions indicate the depths at which alteration minerals were directly observed in thin section, while gray regions indicate regions suitable for mineral formation but without direct observation.

texture as well as grain size and color. Additionally, small amounts of dachiardite are observed in the matrix of some green vein-bearing sections, indicating diffuse orange alteration in these regions. Therefore, it is unlikely that lithology of the host rock is responsible for the observed difference in vein mineralogy.

One hypothesis is that changes in hydrothermal fluid chemistry are responsible. Dachiardite-Na deposition in the veins might be controlled by the sodium content of the circulating fluid. As such, dachiardite-rich orange veins may represent briny conditions, while dachiardite-poor green veins may represent a dilution of the brine by seawater penetration into the upper portion of the impactite sequence. An analysis of fluid inclusions in the core might yield answers to this hypothesis.

The degree of diffuse orange alteration may be affected by breccia physical properties. The largest, densest pockets of diffuse alteration occur between core sections 60-1 and 64-2, which is characterized by a larger clast size, increased clast heterogeneity, and a mottled green matrix color in contrast with the smaller, more uniform clasts and gray matrix of above sections.

Conclusion: Green and orange veins are found in distinct regions of the core with no overlap. No lithological transitions were observed in the region separating the green and orange veins, thus indicating that the host rock is not the controlling factor for vein mineralogy. Diffuse dachiardite alteration occurs in both sections of core. While it does not obviously cross-cut green veins in the uppermost section, its presence may indicate a change in sea water drawdown as the hydrothermal system evolved.

References: [1] Hildebrand A. R. (1991) *Geology, 19*, 867–871. [2] Kring D. A. (1995) *JGR*, *100*, 16979–16986. [3] Abramov A. & Kring D. A. (2007) *MAPS*, *42*, 93–112. [4] Kring D. A. et al. (2020) *Sci. Adv.*, *6*, 9p., eaaz3053. [5] Christeson G. L. et al. (2018) *EPSL, 495*, 1–11. [6] Riller U. et al. (2018) *Nature, 562*, 511–518. [7] Rae A. S. P. et al. (2019) *JGR–Planets, 124*, 1960–1978. [8] Ames D. E. et al. (2004) *MAPS, 39*, 1145–1167. [9] Hecht L. et al. (2004) *MAPS, 39*, 1169–1186. [10] Lüders V. & Rickers K. (2004) *MAPS, 39*, 1187–1197. [11] Rowe A. J. et al. (2004) *MAPS, 39*, 1223–1231. [12] Nelson M. J. et al. (2012) *GCA*, *86*, 1–20. [13] J. V. Morgan et al. (2016) *Science, 354*, 878–882. [14] Gulick S. et al. (2017) Upper Peak Ring, in *Chicxulub: Drilling the K-Pg Impact Crater*. [15] Ormö J. et al. (2019) *EPSL*, *564*, 116915, 14p.